

Monthly Iceberg Calving Dataset of the Antarctic Ice Shelves (2010–2019)

Qi, M. Z.^{1,3,4} Liu, Y.^{1,3,4} Cheng, X.^{2,3,4*} Feng, Q. Y.¹ Lin, Y. J.^{1,4} Wei, Y.^{1,3,4}
Yang, C.^{1,3,4} Hui, F. M.^{2,3,4} Chen, Z. Q.^{2,3,4} Li, X. Q.^{2,3,4} Zhang, Y. Y.^{1,3,4}
Zhang, Y.^{1,3,4} Chen, X. T.^{1,4} Liu, A. B.^{1,3,4} Chen, Y. T.^{1,3,4} Guan, Z. F.^{1,4} Ye,
Y.^{1,4} Shang, X. Y.^{1,3,4} Tian, J. H.^{1,3,4} Duan, M. H.^{1,4} Zhang, Z. Y.^{1,3,4}

1. State Key Laboratory of Remote Sensing Science, and College of Global Change and Earth System Science, Beijing Normal University, Beijing 100875, China;
2. School of Geospatial Engineering and Science, Sun Yat-Sen University, Zhuhai 519082, China;
3. Southern Marine Science and Engineering Guangdong Laboratory, Zhuhai 519082, China;
4. University Corporation for Polar Research, Beijing 100875, China

Abstract: Iceberg calving is a major process of Antarctic mass loss, and it has been regarded as a crucial variable in precisely evaluating the mass balance of ice shelves. We used multi-source remote sensing data from the first three days of each month from August 2010 to August 2019, including ENVISAT ASAR (WSM) images from August 2010 to April 2012, Terra/Aqua MODIS 7-2-1 band composite images from January 2012 to December 2014 (except during polar night), Landsat-8 OLI 4-3-2 band composite images from October 2013 to August 2019 (except during polar night), and Sentinel-1 SAR (EW) images from October 2014 to August 2019, to generate monthly mosaics of the Antarctic coastline. Then, combining the image data with the annual iceberg calving dataset, we extracted all monthly calving events that occurred between August 2010 and August 2019 through vector segmentation and calculated the area, thickness, mass, and calving period through spatial computing. The monthly iceberg calving dataset of the Antarctic ice shelves, which were classified by month (12 monthly datasets and one polar night dataset), contains the distribution of each monthly calving event, along with the calving year, calving month, length, area, thickness, mass, calving period, and calving type. This dataset is archived in .shp format and consists of 104 data files with a data size of 4.3 MB (compressed to one file, 1.6 MB).

Keywords: Antarctica; ice shelves; iceberg calving; remote sensing; 2010–2019

Dataset Availability Statement:

The dataset supporting this paper was published and is accessible through the *Digital Journal of Global Change Data Repository* at: <https://doi.org/10.3974/geodb.2020.04.13.V1>.

Received: 30-06-2020; **Accepted:** 28-08-2020; **Published:** 25-09-2020

Foundations: Ministry of Science and Technology of P. R. China (2018YFA0605403); National Natural Science Foundation of China (41925027)

Corresponding Author: Cheng, X. AAT-6307-2020, School of Geospatial Engineering and Science, Sun Yat-Sen University, chengxiao9@mail.sysu.edu.cn

Data Citation: [1] Qi, M. Z., Liu, Y., Cheng, X., *et al.* Monthly iceberg calving dataset of the Antarctic ice shelves (2010–2019) [J]. *Journal of Global Change Data & Discovery*, 2020. <https://doi.org/10.3974/geodp.2020.03.01>.

[2] Qi, M. Z., Liu, Y., Cheng, X., *et al.* Monthly iceberg calving dataset of the Antarctic ice shelves (2010–2019) [J/DB/OL]. *Digital Journal of Global Change Data Repository*, 2020. <https://doi.org/10.3974/geodb.2020.04.13.V1>.

1 Introduction

Iceberg calving, the shedding of ice from an ice shelf or the frontal edge of a glacier into the ocean, is one of the main processes of Antarctic ice mass loss^[1–3]. Observations of individual calving events with high spatial and temporal resolution are important in optimizing existing ice sheet models^[4–5], further studying the triggering mechanisms of calving^[6], and better understanding the behaviours of glaciers and ice sheets^[7]. Monitoring individual calving events at the continental scale month by month is time-consuming and laborious; therefore, current studies of Antarctic iceberg calving have focused more on small scales or specific ice shelves^[8–9], and there is still a lack of high-precision monitoring of monthly calving events over long periods.

Based on the annual iceberg calving product and multisource satellite imagery of the Antarctic ice shelves^[10], this dataset was developed after artificial interpretation and spatial editing. This dataset contains attributes of each monthly calving event from August 2010 to August 2019, including their locations, outlines, years of occurrence, months of occurrence, areas, thicknesses, masses, cycles, and types. The minimum extracted area of calving is approximately 0.02 km², and the temporal resolution is monthly. The monthly iceberg calving dataset can be used not only to reflect the local details of monthly iceberg calving but also as a basis for spatial analysis of seasonal patterns of calving at different scales.

2 Metadata of the Dataset

The metadata of the “Monthly iceberg calving dataset of the Antarctic ice shelves (2010–2019)”^[11] are shown in Table 1.

Table 1 Metadata summary of the “Monthly iceberg calving dataset of the Antarctic ice shelves (2010–2019)”

Items	Description
Dataset full name	Monthly iceberg calving dataset of the Antarctic ice shelves (2010–2019)
Dataset short name	MonthlyIcebergCalvingAntarctic_2010-2019 Authors As shown in Table 2
Geographical region	Antarctica Year From August 2010 to August 2019
Temporal resolution	1 month Spatial resolution 0.02 km ²
Data format	.shp
Data size	4.3 MB (compresses to one file, 1.6 MB)
Data files	This dataset provides monthly calving events occurring across the Antarctic ice shelf over nine consecutive years and consists of 12 monthly iceberg calving sub-datasets and one polar night calving sub-dataset, with each subset named by the month (or polar night). The subset contains information on the specific years in which the monthly disintegrations occurred, as shown in Table 3
Foundations	Ministry of Science and Technology of P. R. China (2018YFA0605403); National Natural Science Foundation of China (41925027)
Data publisher	Global Change Scientific Research Data Publishing System, http://www.geodoi.ac.cn
Address	11A, Datun Road, Chaoyang District, Beijing 100101, China
Data sharing policy	Data from the Global Change Research Data Publishing & Repository includes metadata, datasets (in the <i>Digital Journal of Global Change Data Repository</i>), and publications (in the <i>Journal of Global Change Data & Discovery</i>). Data sharing policy includes: (1) Data are openly available and can be free downloaded via the Internet; (2) End users are encouraged to use Data subject to citation; (3) Users, who are by definition also value-added service providers, are welcome to redistribute Data subject to written permission from the GCdataPR Editorial Office and the issuance of a Data redistribution license; and (4) If Data are used to compile new datasets, the ‘ten per cent principal’ should be followed such that Data records utilized should not surpass 10% of the new dataset contents, while sources should be clearly noted in suitable places in the new dataset ^[12]
Communication and searchable system	DOI, DCI, CSCD, WDS/ISC, GEOSS, China GEOSS, Crossref

Table 2 Authors' information on the dataset

No.	Name	Research ID	Department	E-mail
1	Qi, M. Z.	AAT-5417-2020	College of Global Change and Earth System Science, Beijing Normal University	201921490035@mail.bnu.edu.cn
2	Liu, Y.	AAT-5481-2020	College of Global Change and Earth System Science, Beijing Normal University	liuyan2013@bnu.edu.cn
3	Cheng, X.	AAT-6307-2020	School of Geospatial Engineering and Science, Sun Yat-Sen University	chengxiao9@mail.sysu.edu.cn
4	Feng, Q. Y.	AAT-5443-2020	College of Global Change and Earth System Science, Beijing Normal University	306592082@qq.com
5	Lin, Y. J.	AAT-6421-2020	College of Global Change and Earth System Science, Beijing Normal University	201921490033@mail.bnu.edu.cn
6	Wei, Y.	AAT-5411-2020	College of Global Change and Earth System Science, Beijing Normal University	201721490021@mail.bnu.edu.cn
7	Yang, C.	AAT-5429-2020	College of Global Change and Earth System Science, Beijing Normal University	201821490039@mail.bnu.edu.cn
8	Hui, F. M.	AAT-5865-2020	School of Geospatial Engineering and Science, Sun Yat-Sen University	huifm@mail.sysu.edu.cn
9	Chen, Z. Q.	0000-0003-0131-3132 (ORCID)	School of Geospatial Engineering and Science, Sun Yat-Sen University	chenzq_2019@163.com
10	Li, X. Q.	AAT-5475-2020	School of Geospatial Engineering and Science, Sun Yat-Sen University	lixq85@mail.sysu.edu.cn
11	Zhang, Y. Y.	J-5625-2017	College of Global Change and Earth System Science, Beijing Normal University	yyzhang@mail.bnu.edu.cn
12	Zhang, Y.	AAT-5442-2020	College of Global Change and Earth System Science, Beijing Normal University	–
13	Chen, X. T.	AAT-6570-2020	College of Global Change and Earth System Science, Beijing Normal University	–
14	Liu, A. B.	AAT-5467-2020	College of Global Change and Earth System Science, Beijing Normal University	–
15	Chen, Y. T.	AAT-5592-2020	College of Global Change and Earth System Science, Beijing Normal University	–
16	Guan, Z. F.	AAT-6298-2020	College of Global Change and Earth System Science, Beijing Normal University	–
17	Ye, Y.	AAT-6591-2020	College of Global Change and Earth System Science, Beijing Normal University	–
18	Shang, X. Y.	AAT-5505-2020	College of Global Change and Earth System Science, Beijing Normal University	–
19	Tian, J. H.	AAT-5892-2020	College of Global Change and Earth System Science, Beijing Normal University	–
20	Duan, M. H.	AAT-5952-2020	College of Global Change and Earth System Science, Beijing Normal University	–
21	Zhang, Z. Y.	AAT-6574-2020	College of Global Change and Earth System Science, Beijing Normal University	–

3 Methods

A monthly calving event is defined as an independent calved area in the monthly cycle that is not spatially adjacent to other calving events that occurred in the same month of the year. That is, all monthly calving polygons in the same year and month are required to be spatially non-overlapping and non-adjacent, with each record representing an independent monthly calving event^[2, 13]. In this section, the data and methods used during the development of this dataset will be introduced.

3.1 Data Sources

Satellite imagery: Images of the first three days of each month from August 2010 to August 2019 were preferentially selected as the basis for determining the month in which calving occurred. Satellite imagery coverage is shown in Figure 1.

Month Year	January	February	March	April	May	June	July	August	September	October	November	December
2010								ENVISAT ASAR (WSM)				
2011	ENVISAT ASAR (WSM)											
2012	ENVISAT ASAR (WSM); Terra/Aqua MODIS			Polar night (Data missing)					Terra/Aqua MODIS			
2013	Terra/Aqua MODIS								Terra/Aqua MODIS; Landsat-8 OLI			
2014	Terra/Aqua MODIS; Landsat-8 OLI								Terra/Aqua MODIS; Landsat-8 OLI; Sentinel-1 SAR (EW)			
2015	Sentinel-1 SAR (EW); Landsat-8 OLI											
2016	Sentinel-1 SAR (EW); Landsat-8 OLI											
2017	Sentinel-1 SAR (EW); Landsat-8 OLI											
2018	Sentinel-1 SAR (EW); Landsat-8 OLI											
2019	Sentinel-1 SAR (EW); Landsat-8 OLI											

Figure 1 Satellite imagery used in the development of the “Monthly iceberg calving dataset of the Antarctica ice shelves (2010–2019)”

The ENVISAT satellite was launched by the ESA (European Space Agency). The ASAR (Advanced Synthetic Aperture Radar) sensor operates in the C-band with a central frequency of 5.331 GHz, an ASAR WSM imaging width of 400 km, a spatial resolution of 150 m, and a geospatially encoded pixel pitch of 75 m^[14]. The Sentinel-1 satellite was also launched by the ESA. The dual satellite systems have a revisit period of fewer than 6 days at high latitudes. Both satellites carry a dual-polarized C-band SAR sensor with a centre frequency of 5.405 GHz. The EW mode is suitable for regions requiring extensive coverage, such as the polar regions, with an imaging width of 400 km and a spatial resolution of 40 m^[15]. The Terra and Aqua satellites were launched by NASA and contain 36 channels of MODIS (Moderate Resolution Imaging Spectroradiometer) sensors with a spectral range of 0.4–14.4 µm, a revisit period of 1–2 days, and an imaging width of 2,330 km. The spatial resolution of moonless products synthesized from Antarctic MODIS (7-2-1 band) reflectance images is 250 m, based on Antarctic MODIS (7-2-1 band) daily reflectance image production^[16]. The Landsat-8 satellite was also launched by NASA; the revisit period was 16 days. The OLI (Operational Land Imager) sensor has an imaging width of 190 km and the multispectral band spatial resolution of 30 m^[17].

Other reference data include the annual iceberg calving dataset of the Antarctic ice shelf (2005–2019)^[10]. This dataset records the location and outline of all annual calving events occurring on the Antarctic ice shelf larger than 1 km² from August 2005 to August 2019 in shapefile format and provides information on the area, perimeter, average thickness, mass, recurrence cycle, type of calving, and year of occurrence in the attribute table. The time resolution of the dataset is annual.

3.2 Technical Route

The development of the monthly iceberg calving dataset can be divided into two steps: image preprocessing and iceberg calving monitoring, as shown in Figure 2. Image pre-processing includes geocoding, geometric correction, and mosaic production. The pre-processing yields the Antarctic coastline mosaic at an early date of each month. The

iceberg calving monitoring includes month determination, calved area segmentation, and attribute updating. For each annual calving event, the images of each month are traversed to determine the calving condition of each month, and then the annual calving events are segmented according to the actual month of calving (Figure 3), after the vector of the monthly calved area is obtained.

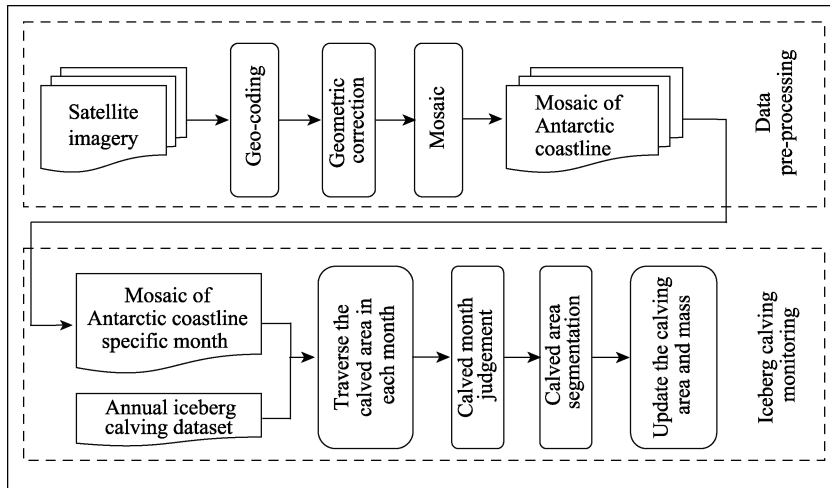


Figure 2 Flow chart of the dataset development for monitoring monthly iceberg calving events

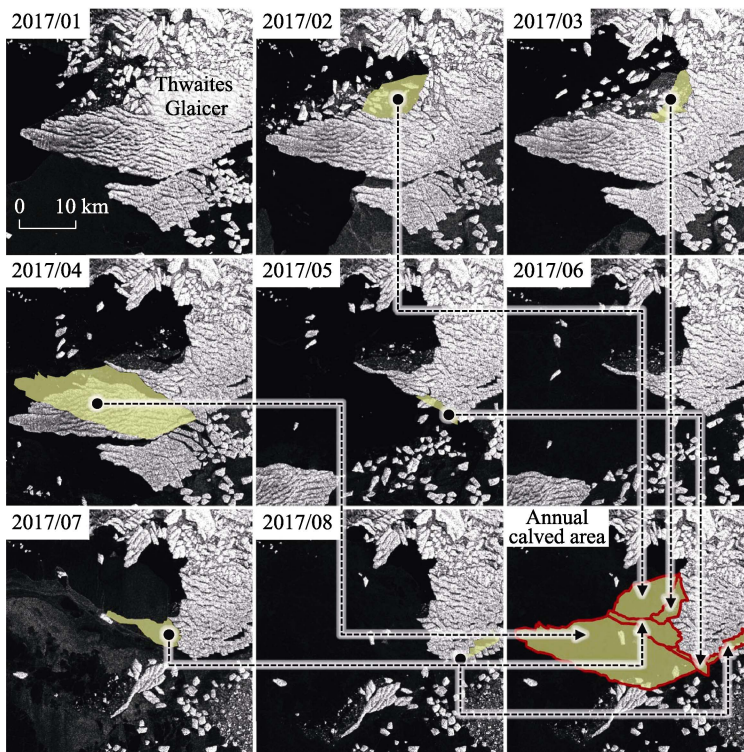


Figure 3 Schematic of the extraction process of monthly calving events

4 Data Results and Validation

4.1 Data Products

The minimum iceberg calving polygon in the monthly iceberg calving dataset is approximately 0.02 km². The time range is from August 2010 to August 2019, and the data file is archived in .shp format. The dataset consists of a subset of Antarctic iceberg calving data for 13 intervals (12 months and one polar night of 2012–2014) and contains 104 data files, totaling 1,774 data records. Calving events did not occur in every month of each year. The detailed information of the subset of the monthly calving dataset in this product and its specific year of occurrence is described in Table 3. Table 4 shows the descriptions of the fields in the dataset attribute table.

Table 3 Information on monthly calving data files of the monthly iceberg calving of the Antarctic ice shelf

No.	Filename	Description
1	Calving_January	Contains calving events in January of each year from 2011 to 2019
2	Calving_February	Contains calving events in February of each year from 2011 to 2019
3	Calving_March	Contains calving events in March of each year from 2011 to 2019
4	Calving_April	Contains calving events in April of each year from 2011 to 2013 and 2015 to 2019
5	Calving_May	Contains calving events in May of 2011 and each year from 2015 to 2019
6	Calving_June	Contains calving events in June of each year from 2015 to 2019
7	Calving_July	Contains calving events in July of each year from 2015 to 2019
8	Calving_August	Contains calving events in August of each year from 2011 to 2012 and 2014 to 2018
9	Calving_September	Contains calving events in September of each year from 2011 to 2018
10	Calving_October	Contains calving events in October of each year from 2011 to 2013 and from 2015 to 2018
11	Calving_November	Contains calving events in November of each year from 2010 to 2018
12	Calving_December	Contains calving events in December of each year from 2010 to 2018
13	Calving_PolarNight	Contains calving events during the polar night (from May to August) in 2011, 2012, and 2013. Due to image quality limitations, it is not possible to determine the exact month in which the calving occurred

Table 4 Description of the attribute of the monthly iceberg calving dataset

No.	Name	Unit	Description
1	Id	–	ID of the calving polygons
2	Year	year	The year interval in which the calving occurred (for example, 2015–2016 represents the year it occurred between August 2015 and August 2016)
3	Month	month	The month in which the calving occurred
4	Year_Mon	–	The month and year in which the calving occurred (the first four digits represent the year, the last two the month)
5	Length	km	The perimeter of the calved area
6	Area	km ²	The area of the calving event
7	Size	–	Calving scale (according to the calved area, 0 stand for tiny-scale calving smaller than 1 km ² , 1 for small-scale calving with an area between 1 and 10 km ² , 2 for medium-scale calving with an area between 10 and 100 km ² , 3 for large-scale calving with an area between 100 and 1,000 km ² , 4 for extra-large-scale calving with an area larger than 1,000 km ²)
8	Thickness	km	The average thickness of the calved area
9	Mass	Gt	The mass of the calved area
10	Cycle	year	The calving recurrence interval which comes from the original annual calving event
11	Type	–	The type of calving which comes from the original annual calving event
12	H_from	–	Data source of the thickness

4.2 Data Analysis

The frequency of calving of the Antarctic ice shelf shows a clear seasonal pattern, with calving concentrated mainly in the austral summer (from December to March) and autumn (from April to June); calving events in these seasons accounted for 66.9% of the total calving frequency. The frequency of calving was highest in February, followed by January and March (26.4%, 22.3%, and 18.2%, respectively), and was the lowest in July (only 1.7%). The area of calving and the quality of calving also showed a seasonal distribution, with a monthly increase from December to March, a decrease in April, a minimum in June, and a small peak in October. An unusual peak in July was attributed to the extra-large calving of the Larsen C Ice Shelf, with an area larger than 6,000 km² and a mass of more than 1,100 Gt, in July 2016.

The frequency, area, and mass distributions of monthly calving events at different scales weakened in their seasonal patterns as the scale increased. As shown in Figure 4, the frequency of small- and medium-sized calving events was highest in February, and the seasonal trends were similar for the three scales, with the frequency of calving remaining stable and low between April and October. Similarly, the area and mass of small- and medium-sized calving events exhibited seasonal characteristics similar to the frequency distribution. The area and mass of large calving events were generally high during the austral summer, but high values were also observed in other months. Extra-large calving events occurred only twice during the observation period, and their seasonal distribution is not yet known.

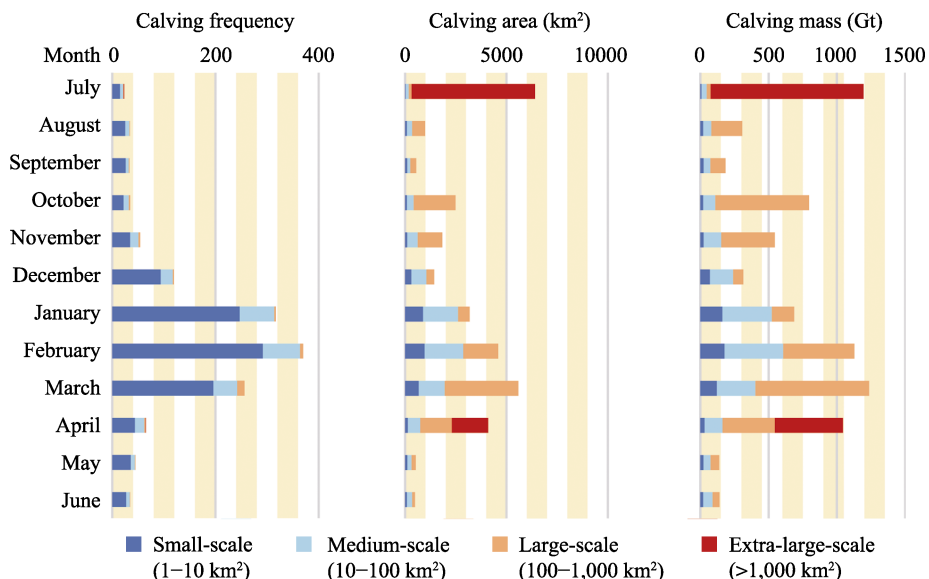


Figure 4 Distribution of the frequencies, areas, and masses of monthly iceberg calving events at different scales (2010–2019)

The annual frequencies, areas, and mass ratios of the small, medium, and large monthly calving events were relatively stable. As shown in Figure 5, the highest frequency of small calving events was approximately 60%. The highest percentages of small- and medium-sized calving events both occurred in January, accounting for 26.8% and 54.3% of the

total area, respectively. The month with the highest percentage of large calving areas was March, at 64.9%. The distribution and trend of the proportion of calving mass were similar to that of the calving area.

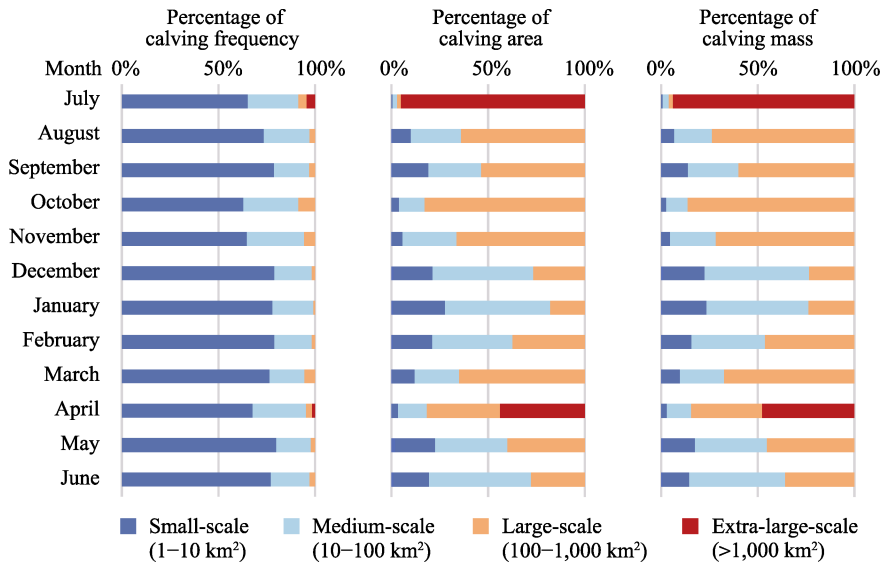


Figure 5 Ratio distribution of frequency, area, and mass of monthly iceberg calving at different scales (2010–2019)

The spatial distribution of the monthly calving of the Antarctic ice shelf from 2010 to 2019 is shown in Figure 6. Small-scale calving events covered the largest area in January–March when calving events are frequent. In other months, small- and medium-sized calving events remained most frequent in West Antarctica, followed by the east of the Amery Ice Shelf in East Antarctica. Few calving events occurred in the west of the Amery Ice Shelf in East Antarctica. Large calving events were relatively frequent in West Antarctica during the observation time interval, with large calving events in February concentrated in West Antarctica and the Wilkes Land in East Antarctica, but with large calving events in March scattered across Antarctica. Extra-large calving events occurred only twice, once in July on the Larsen C Ice Shelf in the Antarctic Peninsula, and once in April on the Thwaites Ice Shelf in West Antarctica, respectively.

4.3 Data Validation

The monthly calving area was obtained by splitting the annual calving area, so the accuracy of the Antarctic ice shelf monthly calving dataset inherits the extraction accuracy of the annual calving area. The equivalent perimeter of the calving zone area observation error is 5 m, and the area observation error is 5 times the calving zone perimeter (m²). The area of a single monthly calving event is smaller than or equal to its corresponding annual calving event, so its area observation error is smaller than the area observation error of the annual calving event; i.e., the annual average calving zone area observation error is less than 17.1 km².

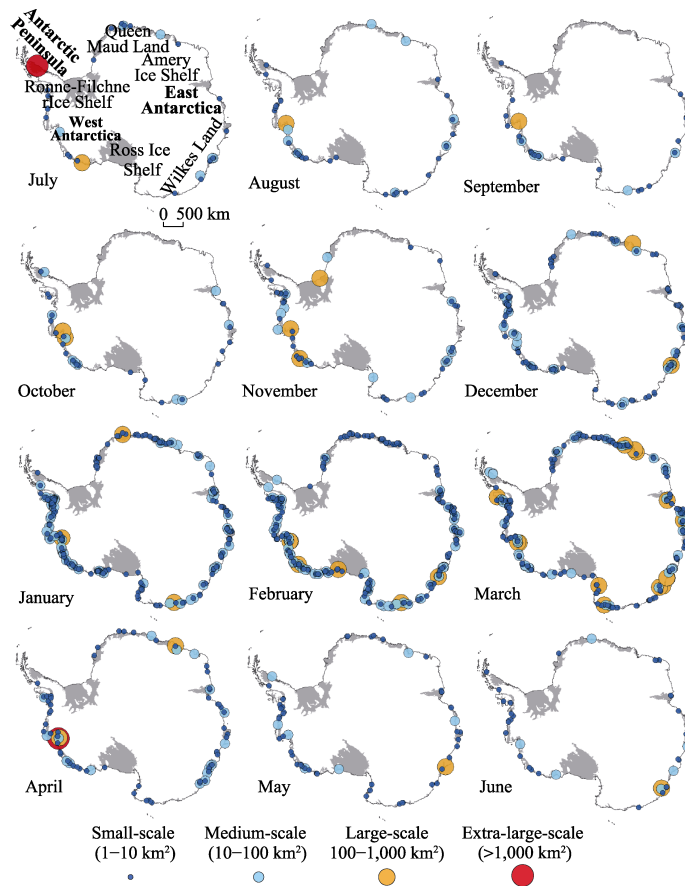


Figure 6 Cumulative distribution of monthly iceberg calving at different scales (2010–2019)

5 Discussion and Conclusion

Based on the multisource optical and synthetic aperture radar (SAR) data covering the Antarctic coastline month by month from 2010 to 2019, we first developed the monthly iceberg calving dataset of the Antarctic ice shelves (2010–2019) to provide detailed monitoring of the monthly calving events of the circum-Antarctic ice shelf for nine consecutive years and to quantitatively assess the seasonal characteristics of the calving of the Antarctic ice shelf.

Based on this dataset, we preliminarily analysed the relationship between the monthly calving of the Antarctic ice shelf and the ice sheet surface melting^[18] and Antarctic sea ice area^[19]. The results show that the frequency of monthly iceberg calving events and the maximum surface melt area of the ice sheet had similar trends, which were positive but not significantly correlated. The peak of calving occurred in February, while the peak of ice-sheet surface melting occurred in January. The frequency of monthly calving of the Antarctic ice shelf was significantly negatively correlated with the trend of the Antarctic monthly sea ice area. The most frequent calving occurred in February when the sea ice area was at its minimum.

Author Contributions

Cheng, X., Liu, Y., Qi, M. Z., Hui, F. M., and Chen, Z. Q. designed the dataset. Qi, M. Z., Feng, Q. Y., Li, X. Q., Zhang, Y. Y., Zhang, Y., Chen, X. T., Liu, A. B., Chen, Y. T., Guan,

Z. F., YE, Y., Shang, X. Y., Tian, J. H., Duan, M. H., and Zhang, Z. Y. collected and pre-processed the remotely sensed data. Qi, M. Z., Feng, Q. Y., Lin, Y. J., Wei, Y., and Yang, C. extracted the monthly iceberg calving events. Liu, Y., and Qi, M. Z. were in charge of the model design and algorithm. Qi, M. Z. performed data validation. Qi, M. Z. and Liu, Y. wrote the data paper.

References

- [1] Depoorter, M. A., Bamber, J. L., Griggs, J. A., *et al.* Calving fluxes and basal melt rates of Antarctic ice shelves [J]. *Nature*, 2013, 502(7469): 89–92.
- [2] Liu, Y., Moore, J. C., Cheng, X., *et al.* Ocean-driven thinning enhances iceberg calving and retreat of Antarctic ice shelves [J]. *Proceedings of the National Academy of Sciences of the United States of America*, 2015, 112(11): 3263–3268.
- [3] Rignot, E., Jacobs, S., Mouginot, J., *et al.* Ice-shelf melting around Antarctica [J]. *Science*, 2013, 341(6143): 266–70.
- [4] Massom, R. A., Scambos, T. A., Bennetts, L. G., *et al.* Antarctic ice shelf disintegration triggered by sea ice loss and ocean swell [J]. *Nature*, 2018, 558(7710): 383–389.
- [5] Pattyn, F., Morlighem, M. The uncertain future of the Antarctic Ice Sheet [J]. *Science*, 2020, 367(6484): 1331–1335.
- [6] Medrzycka, D., Benn, D., Box, J., *et al.* Calving Behavior at Rink Isbræ, West Greenland, from Time-Lapse Photos [J]. *Arctic, Antarctic, and Alpine Research*, 2016, 48(2): 263–277.
- [7] Åström, J. A., Vallot, D., Schäfer, M., *et al.* Termini of calving glaciers as self-organized critical systems [J]. *Nature Geoscience*, 2014, 7(12): 874–878.
- [8] Wahlin, A. K., Steiger, N., Darelius, E., *et al.* Ice front blocking of ocean heat transport to an Antarctic ice shelf [J]. *Nature*, 2020, 578(7796): 568–571.
- [9] Darelius, E., Fer, I., Nicholls, K. W. Observed vulnerability of Filchner-Ronne Ice Shelf to wind-driven inflow of warm deep water [J]. *Nature Communications*, 2016, 7: 12300.
- [10] Qi, M. Z., Liu, Y., Cheng, X., *et al.* Annual iceberg calving dataset of the Antarctic ice shelves (2005–2019) [J/DB/OL]. *Digital Journal of Global Change Data Repository*, 2020. <https://doi.org/10.3974/geodb.2020.04.09.V1>.
- [11] Qi, M. Z., Liu, Y., Cheng, X., *et al.* Monthly iceberg calving dataset of the Antarctic ice shelves (2010–2019) [J/DB/OL]. *Digital Journal of Global Change Data Repository*, 2020. <https://doi.org/10.3974/geodb.2020.04.13.V1>.
- [12] GCdataPR Editorial Office. GCdataPR data sharing policy [OL]. <https://doi.org/10.3974/dp.policy.2014.05> (Updated 2017).
- [13] Liu Y., Cheng X., Hui, F. M., *et al.* Antarctic iceberg calving monitoring based on EnviSat ASAR images [J]. *Journal of Remote Sensing*, 2013, 17(3): 479–494.
- [14] ENVISAT ASAR WSM [DB/OL]. <http://eogrid.esrin.esa.int/browse>.
- [15] Sentinel-1 SAR EW [DB/OL]. <https://www.esa.int/ESA>.
- [16] Terra Aqua MODI [DB/OL]. <https://worldview.earthdata.nasa.gov/>.
- [17] Landsat-8 OLI [DB/OL]. <https://www.usgs.gov/>.
- [18] Picard, G., Fily, M. Surface melting observations in Antarctica by microwave radiometers: correcting 26-year time series from changes in acquisition hours [J]. *Remote Sensing of Environment*, 2006, 104(3): 325–336.
- [19] Stroeve, J., Meier, W. N. Sea ice trends and climatologies from SMMR and SSM/I-SSMIS (version 3) [Z]. NASA National Snow and Ice Data Center Distributed Active Archive Center, 2018.